



HAL
open science

Energetics of a uranothorite ($\text{Th}_{1-x}\text{U}_x\text{SiO}_4$) solid solution

Xiaofeng Guo, Stephanie Szenknect, Adel Mesbah, Nicolas Clavier, Christophe Poinssot, Di Wu, Hongwu Xu, Nicolas Dacheux, Rodney Ewing, Alexandra Navrotsky

► To cite this version:

Xiaofeng Guo, Stephanie Szenknect, Adel Mesbah, Nicolas Clavier, Christophe Poinssot, et al.. Energetics of a uranothorite ($\text{Th}_{1-x}\text{U}_x\text{SiO}_4$) solid solution. *Chemistry of Materials*, 2016, 28 (19), pp.7117-7124. <10.1021/acs.chemmater.6b03346>. <hal-02045481>

HAL Id: hal-02045481

<https://hal.science/hal-02045481v1>

Submitted on 20 Sep 2024

HAL is a multi-disciplinary open access archive for the deposit and dissemination of scientific research documents, whether they are published or not. The documents may come from teaching and research institutions in France or abroad, or from public or private research centers.

L'archive ouverte pluridisciplinaire HAL, est destinée au dépôt et à la diffusion de documents scientifiques de niveau recherche, publiés ou non, émanant des établissements d'enseignement et de recherche français ou étrangers, des laboratoires publics ou privés.



HAL Authorization

LA-UR-16-26227 (Accepted Manuscript)

Energetics of a Uranothorite ($\text{Th}_{1-x}\text{U}_x\text{SiO}_4$) Solid Solution

Guo, Xiaofeng
Szenknect, Stephanie
Mesbah, Adel
Clavier, Nicolas
Poinssot, Christophe
Wu, Di
Xu, Hongwu
Ewing, Rodney C.
Navrotsky, Alexandra

Provided by the author(s) and the Los Alamos National Laboratory (2017-01-11).

To be published in: Chemistry of Materials

DOI to publisher's version: 10.1021/acs.chemmater.6b03346

Permalink to record: <http://permalink.lanl.gov/object/view?what=info:lanl-repo/lareport/LA-UR-16-26227>

Disclaimer:

Approved for public release. Los Alamos National Laboratory, an affirmative action/equal opportunity employer, is operated by the Los Alamos National Security, LLC for the National Nuclear Security Administration of the U.S. Department of Energy under contract DE-AC52-06NA25396. Los Alamos National Laboratory strongly supports academic freedom and a researcher's right to publish; as an institution, however, the Laboratory does not endorse the viewpoint of a publication or guarantee its technical correctness.

Energetics of Uranothorite ($\text{Th}_{1-x}\text{U}_x\text{SiO}_4$) Solid Solution

Xiaofeng Guo^{1,2}, Stéphanie Szenknect³, Adel Mesbah³, Nicolas Clavier³, Christophe Poinssot⁴, Di Wu⁵, Hongwu Xu¹, Nicolas Dacheux³, Rodney C. Ewing⁶, and Alexandra Navrotsky^{2,*}

¹ Earth and Environmental Sciences Division, Los Alamos National Laboratory, Los Alamos, New Mexico 87545, United States

² Peter A. Rock Thermochemistry Laboratory and NEAT ORU, University of California Davis, Davis, California 95616, United States

³ Institut de Chimie Séparative de Marcoule, ICSM - UMR 5257, CNRS / CEA / University of Montpellier / ENSCM, Site de Marcoule - Bât. 426 BP 17171, 30207 Bagnols sur Cèze cédex, France

⁴ CEA, Nuclear Energy Division, Radiochemistry & Processes Department, BP 17171, 30207 Bagnols sur Cèze, France

⁵ The Gene and Linda Voiland School of Chemical Engineering and Bioengineering, Washington State University, Pullman, Washington 99163, United States

⁶ Department of Geological Sciences, Stanford University, Stanford, California 94305, United States

* e-mail: anavrotsky@ucdavis.edu

Abstract

High-temperature oxide melt solution calorimetric measurements were completed to determine the enthalpies of formation of the uranothorite, $(\text{USiO}_4)_x - (\text{ThSiO}_4)_{1-x}$, solid solution. Phase - pure samples with $x = 0, 0.11, 0.21, 0.35, 0.71,$ and 0.84 were prepared, purified, and characterized by powder X-ray diffraction, electron probe microanalysis, thermogravimetric analysis and differential scanning calorimetry coupled with *in situ* mass spectrometry, and high temperature oxide melt solution calorimetry. This work confirms the energetic metastability of coffinite, USiO_4 , and of U-rich intermediate silicate phases with respect to a mixture of binary oxides. However, variations in unit cell parameters and negative excess volumes of mixing, coupled with strongly exothermic enthalpies of mixing in the solid solution, suggest short-range cation ordering that can stabilize intermediate compositions, especially near $x = 0.5$.

Introduction

Uranothorite ($\text{Th}_{1-x}\text{U}_x\text{SiO}_4$), isomorphic to zircon ($I4_1/amd$), can be prepared in a complete series from thorite (ThSiO_4) to coffinite (USiO_4)¹⁻⁵. Its presence in nature is widespread in uranium deposits⁶⁻¹¹, reflecting direct substitutions between U and Th^{6, 9-11}. The end members coffinite¹² and thorite² are also among the few known naturally occurring actinide orthosilicates^{11, 13, 14}. Despite having the same structure as zircon, they exhibit significant differences in ease of synthesis, geological conditions of formation and grain size. Natural coffinite usually occurs in microcrystals accompanied by uraninite, zircon, sulfides or organic matters^{11, 14-22}. Pure synthetic coffinite is difficult to prepare and purify^{3-5, 23, 24}. Coffinite cannot be made by direct high temperature reaction of UO_2 and SiO_2 but can be synthesized from aqueous precursors over a limited pH range in the presence of carbonate buffer²⁵, where the formation of uranium hydroxosilicate colloids may play an important role in forming the fine-grained (often nanoscale) coffinite that might be thermodynamically stabilized by structural water or (OH)^{-25, 26}. Thorite, on the other hand, occurs as well crystallized macroscopic primary or an accessory mineral in igneous and metamorphic rocks.^{11, 15} Thorite is easily synthesized¹, even by direct reaction of ThO_2 and SiO_2 .^{27, 28} These differences in the ease of synthesis and typical grain-sizes obtained reflect differences in their thermodynamic stability.

Recent thermodynamic studies have demonstrated that coffinite is metastable. Guo *et al.*²⁶, using oxide melt solution calorimetry, reported the standard enthalpy of formation of coffinite from elements to be -1970.0 ± 4.2 kJ/mol and its enthalpy of formation from oxides to be 25.6 ± 3.9 kJ/mol. This latter significantly positive value strongly suggests metastability of coffinite with respect to the binary oxides.²⁶ Szenknect *et al.* measured the standard Gibbs free energy of formation to be -1872 ± 6 kJ/mol⁵ or, most recently, -1867.6 ± 3.2 kJ/mol²⁹, and the solubility constant of coffinite at 25 °C and 1 bar to be -5.25 ± 0.05 ²⁹. These data confirm that coffinite is

metastable relative to uraninite and quartz. The enthalpy of formation of thorite from oxides was previously reported by Mazeina *et al.* to be 19.6 ± 2.0 kJ/mol³⁰, but in this work, see below, it has been remeasured to be -6.4 ± 5.7 kJ/mol, suggesting thorite may be thermodynamically stable with respect to ThO₂ and SiO₂, consistent with its direct synthesis from thorianite plus quartz.

Uranothorite, as a bridging composition between thorite to coffinite and may be expected to show intermediate synthetic, structural and thermodynamic features. Szenknect *et al.*⁵ used a series of uranothorites ($x = 0$ to ~ 0.5) to extrapolate the formation energetics of coffinite and confirmed the metastability of USiO₄. Costin *et al.*⁴ explained the difficulty of coffinite synthesis by showing the increased difficulty of preparing pure uranothorites with high uranium loadings. Clavier *et al.*³¹ and Labs *et al.*²⁴ have described the effect of compositional changes on unit cell dimensions and bond-lengths in uranothorite.

Uranothorite may have potential applications as a nuclear waste form or as an alteration product of U-Th nuclear fuels. The zircon structure was proposed as a nuclear waste form^{1, 28} and as a principal phase in inert matrix fuels^{16, 27}. Thus the determination of solubility, chemistry and thermodynamics of actinides, including plutonium, in the zircon structure is of crucial interest^{14, 32-34}. Th⁴⁺ as a Pu⁴⁺ surrogate in uranothorite can provide some insight into the synthesis and thermodynamics of Pu⁴⁺ forming solid solutions with U⁴⁺, where the latter is usually incorporated through coffinitization during spent nuclear fuel alteration in silica-rich fluids^{14, 16, 17, 35-41}. Furthermore, the phase transition of ThSiO₄ from thorite to huttonite at ~ 1200 °C⁴² raises the possibility of a similar phase transition when uranothorite is heated. Huttonite has been suggested to have some advantages over the zircon structure as a nuclear waste form, due to the better performance of monazite (isostructural to huttonite)⁴³ in terms of radiation tolerance and aqueous durability⁴⁴⁻⁴⁶.

Despite the wide interest and potential importance of uranothorite, little has reported on its thermodynamic properties. Ferriss *et al.*³⁴ obtained the enthalpy of mixing by simulations and suggested possible phase separation due to the size difference of U and Th cations. Szenknect *et al.*⁵ obtained the Gibbs free energy of formation up to $x = 0.5$. In the present investigation, thanks to the successful preparation of a complete series of uranothorite compositions, $\text{Th}_{1-x}\text{U}_x\text{SiO}_4$ ($x = 0, 0.11, 0.21, 0.35, 0.71, \text{ and } 0.84$) by hydrothermal reactions, thermodynamic studies can be directly completed on the different pure phase compositions. Specifically, the enthalpies of formation of uranothorite from constituent oxides and from elements were obtained for the first time by high temperature oxide-melt solution calorimetric experiments. The mixing enthalpies of uranothorite solid solutions from coffinite and thorite end members were determined from these enthalpies of solution. The results explain the difficulty of synthesizing single-phase uranothorite with high uranium loadings and demonstrate the metastability of coffinite and U-rich uranothorite solid solution. At intermediate uranium loadings, the solid solutions are somewhat stabilized by a negative heat of mixing suggestive of local cation ordering. These thermodynamic measurements provide for an understanding of U/Th behavior in ore deposits, nuclear fuels, and actinide waste forms.

Experimental Methods

Materials Preparation and Purification

The starting reactants were all supplied by Sigma-Aldrich, except of the depleted uranium turnings, which were provided by CETAMA, France. U(IV) tetrachloride solution was prepared in application of the method proposed by Dacheux *et al.*^{47, 48} consisting of a dissolution of uranium metal in hydrochloride acid (6M). The thorium chloride concentrated solution was obtained by

dissolving thorium nitrate pentahydrate in a 6M HCl solution. Several cycles of evaporation and re-dissolution in a solution of 4M HCl were undertaken until traces of nitrates were eliminated.⁴⁹ The final concentration of both solutions was determined by ICP-AES. To avoid the oxidation of uranium (IV), all the reactions were performed in an argon filled glove box (less than 1 ppm of O₂). Moreover, deionized water was outgassed by boiling approximately for one hour and then cooling under N₂ flow.

Different compositions of the Th_{1-x}U_xSiO₄ series were synthesized by following the procedure reported by Mesbah *et al.*²⁵ and obtained by modification of previous literature methods.^{3, 50} The synthesis consisted of slowly pouring a solution containing the calculated amounts of thorium and uranium into an aqueous solution of Na₂SiO₃ with a molar excess of Si/(U+Th) of about 10 %. The mixture was then made more basic by adding droplets of NaOH (8M) to reach pH values of 11-11.5 and finally buffered by NaHCO₃ to stabilize the pH at 8.7 ± 0.1. The final mixture was transferred into a 23 mL teflon container, placed in a Parr-type acid digestion vessel and then heated in an oven at 250 °C for 7 days. The resulting precipitate was separated from the solution by centrifugation at 4000 rpm, washed twice with water and then with ethanol and dried overnight in air at room temperature.

Despite the optimization of the synthesis procedure, the prepared powders also contained Th_{1-y}U_yO₂ and amorphous SiO₂ as impurities, as noted previously.^{4, 51} To obtain single phase uranorthorite samples, a purification step was performed by following the method reported by Clavier *et al.*²³ consisting of multiple and successive washing cycles in 1M HNO₃, deionized water and then 10⁻² M KOH. Preliminary Raman and FTIR spectroscopy confirmed the formation of pure single phase uranorthorite solid solutions, attested by the absence of the characteristic spectral features of the by-products, such as the T_{2g} vibration mode of actinide dioxides.³¹

Characterization

About 5 mg of each synthesis product was ground into a fine powder and loaded onto a zero-background quartz slide for XRD pattern collection. XRD patterns were collected from 15 to 82 ° (2 θ) with a step size of 0.011° and a collection time of 2 s·step⁻¹ in a Bruker D8 Advance diffractometer with CuK α radiation and a solid-state detector. Chemical compositions and sample homogeneity were determined by electron probe microanalysis (EPMA) using a Cameca SX50 coupled with wavelength dispersive spectrometry (WDS), at an accelerating voltage of 20 keV, a probe current of 10 nA and a spot size of 1 μ m. Quantitative WDS was conducted using a lower accelerating voltage of 15 keV. UO₂, ThO₂, and SiO₂ were used as analytical standards for U, Th, and Si, respectively. Standard Cameca software (PeakSight 4.0 using X-PHI ZAF matrix corrections) was used to calculate the compositions.

Thermal Analysis

Thermogravimetric analysis and differential scanning calorimetry (TG-DSC) were performed simultaneously by heating the sample in a flowing argon atmosphere (40 mL/min) to 800 °C with a rate of 10 °C/min in a Setaram LabSYS simultaneous thermal analyzer. A mass spectrometer (MKS Cirrus2) was connected to detect the released gases. The system was calibrated by decomposing CaC₂O₄. Acquired data were processed with the Calisto software package from AKTS. Detailed procedures have been described previously^{26, 52}.

High Temperature Oxide Melt Solution Calorimetry

High temperature oxide melt solution calorimetry was conducted using a custom built Tian-Calvet twin microcalorimeter⁵³⁻⁵⁵. Powdered samples were hand pressed into small pellets (~5 mg) and were dropped from room temperature into molten solvent (30 g of lead borate (2PbO·B₂O₃)) in a Pt crucible at 802 °C. The calorimeter was calibrated using the heat content of ~ 5 mg α -Al₂O₃ pellets^{53, 54}. O₂ gas was continuously bubbled through the melt at 5 mL/min to ensure an oxidizing environment and facilitate dissolution.⁵⁶ Flushing O₂ gas at ~ 50 mL/min through the calorimeter chamber assisted in maintaining a constant gas environment above the solvent⁵⁶. Upon rapid and complete dissolution of the sample, the enthalpy of drop solution, ΔH_{ds} , was obtained. Dissolution of uranium and thorium oxides and some other uranium containing compounds as well as silica has been demonstrated in this solvent, and drop solution enthalpy data were obtained previously^{26, 52, 57-60}. Finally, using appropriate thermochemical cycles (Table 3), enthalpies of mixing, ΔH_{mix} , enthalpies of formation of the samples from constituent oxides, $\Delta H_{f,ox}$, and standard enthalpies of formation from elements, ΔH°_f , were derived.

Results and Discussion

Based on EPMA and XRD, all of the synthesized and purified uranothorite samples are single-phase and homogeneous, as determined by back scattered electron (BSE) images (Figure 1). Their chemical compositions, determined by WDS, are listed in Table 1. Samples ThU1, ThU2, ThU4, ThU7 and ThU8 have chemical formulae Th_{0.89}U_{0.11}SiO₄, Th_{0.79}U_{0.21}SiO₄, Th_{0.65}U_{0.35}SiO₄, Th_{0.29}U_{0.71}SiO₄ and Th_{0.16}U_{0.84}SiO₄, respectively. The refined unit cell parameters and molar volume of uranothorite are given in Table 2 and Figure 2.

TG/DSC experiments up to 800 °C under an Ar atmosphere (Figure 3) showed that all the samples had good thermal stability, showing no decomposition under these conditions. Powder XRD on the retrieved samples confirmed their zircon structure as in the original samples (Figure 4). The weight losses during heating were due to adsorbed water loss, as confirmed by mass spectroscopy.

In order to avoid any thermal effects from absorbed water during drop solution calorimetric measurements, all samples were annealed at 500 °C to remove the adsorbed water. After annealing, the samples were weighed and immediately dropped into the calorimeter to avoid water reabsorption. The enthalpies of drop solution (ΔH_{ds}) are summarized in Table 4. ΔH_{ds} in a function of uranium content x is plotted in Figure 5a. Its variation fitted by the function (1) suggests a negative deviation from the thermodynamic ideality,

$$\Delta H_{ds} = a + b \cdot x + c \cdot x^2. \quad (1)$$

where $a = 152.0 \pm 3.8$ kJ/mol, $b = -131.9 \pm 17.4$ kJ/mol, $c = -118.7 \pm 17.7$ kJ/mol, and adjusted $R^2 = 0.9989$. This quadratic fit is also supported by the fact that the intercept (152.0 ± 3.8 kJ/mol) is consistent with $\Delta H_{ds}(\text{USiO}_4)$ (154.4 ± 5.4 kJ/mol).

For a description of the energetics of uranothorite solid solutions relative to their end members coffinite and thorite, the enthalpies of mixing, ΔH_{mix} , were derived from the drop solution enthalpies by using the equation:

$$\Delta H_{mix} = - \Delta H_{ds}(\text{Th}_{1-x}\text{U}_x\text{SiO}_4) + x \cdot \Delta H_{ds}(\text{USiO}_4) + (1-x) \cdot \Delta H_{ds}(\text{ThSiO}_4). \quad (2)$$

Values of ΔH_{mix} are plotted in Figure 5b. Because Th ($r_{\text{Th}}^{\text{VIII}} = 1.05$ Å) and U ($r_{\text{U}}^{\text{VI}} = 1.00$ Å) are similar in size, and uranothorite is isostructural with coffinite and thorite, one might expect random substitution of U^{4+} for Th^{4+} in the zircon structure and a close to zero heat of mixing. In

addition, computational results suggest a positive deviation from ideality with a tendency toward exsolution³⁴. However, the experimentally determined heat of mixing curve shows substantial curvature in the opposite direction, with intermediate compositions more energetically stable than a mixture of the two end members (Figure 5b). The heat of mixing can be represented by a quadratic polynomial,

$$\Delta H_{\text{mix}} = \Omega \cdot x(1-x). \quad (3)$$

where Ω is the regular solution parameter that can be obtained by comparing quadratic terms in equation (3) with equation (2) substituted by equation (1): $\Omega = c = -118.7 \pm 17.7$ kJ/mol. The surprising strongly negative value of Ω reflects that the mixing of U and Th in the structure is very exothermic, and the formed intermediate phases are energetically more favorable than the corresponding mechanical mixture of the end members. The relatively small size difference between U (1.00 Å) and Th (1.05 Å) may be a factor that allows for the negative heat of mixing.⁶² Such a strongly negative interaction parameter is suggestive of short-range, cation ordering, which may be most pronounced near $x = 0.5$. The extended X-ray fine structure spectroscopic study by Labs *et al.*²⁴ showed no direct evidence for clustering suggestive of exsolution or for ordering in this complete solid solution.

There may be structural evidence for ordering from the X-ray diffraction refinements. Though previous reports suggested that the unit cell volume decreases linearly as a function of x following Vegard's law^{4, 24, 63}, in this work a careful refinement (Figure 2) indicates significant deviation from Vegard's law behavior. The change in unit cell volume (Figure 2b) is dominated by the change in the **a**-cell parameter. The change of **a** with composition is 2.3 % while that in **c** is only 0.8 %. The **a**-cell parameter shows significant curvature with composition that is reflected in the volume change, while the change in **c** is roughly linear (Figure 2a). Qualitatively, these

changes can be understood in terms of the basic structural features of the zircon structure. The thorite structure consists of two types of chains: ThO₈ polyhedra alternating with SiO₄ tetrahedra that share edges and are parallel to the **c**-axis, and ThO₈ polyhedra that form an edge sharing zig-zag chain parallel to the **a**-axis. Along the **c**-axis, changes that result from the substitution of U *vs.* Th) by simply adjusting the length of the shared edge; hence, the percentage change in the **c**-cell edge is small and essentially reflects the weighted average of the ionic radii of U and Th for each composition. In contrast, along the **a**-axis the U and Th polyhedra share edges and interact directly, and the percentage change in the **a**-parameter is much more sensitive to composition. It is possible that ordering of the U and Th ions can occur such that they alternate in the polyhedra along the chains parallel to the **a**-axis. Maximum order could occur at $x = 0.5$. Since no superstructure has been seen, it is inferred that the ordering is only short range, but it could explain the negative heat of mixing. A full pair distribution function (PDF) analysis of high resolution X-ray or neutron diffraction data could provide a means of detecting short-range order or ordered nanodomains.

The unit cell volume V_{cell} in terms of USiO₄ mole fraction x , is

$$V_{\text{cell}} = a^* + b^* \cdot x + c^* \cdot x^2. \quad (4)$$

where $a^* = 323.3 \pm 0.3 \text{ \AA}^3$, $b^* = -24.8 \pm 1.4 \text{ \AA}^3$, $c^* = 7.7 \pm 1.4 \text{ \AA}^3$, and $\text{adj. } R^2 = 0.9978$ (see Figure 2b). The excess volume or volume of mixing (Figure 2c), is given by $\Delta V_{\text{mix}} = (-7.7 \pm 1.4) \cdot x(1-x) \text{ \AA}^3$ or $(-1.2 \pm 0.2) \cdot x(1-x) \text{ cm}^3/\text{mol}$, and is strongly negative and parallels the enthalpy of mixing in essentially quadratic behavior. The negative enthalpy and volume of mixing are strongly suggestive of local ordering. If such ordering indeed produces a negative volume change, it is possible that high pressure may enhance ordering, even to the point of stabilizing a long range ordered new phase at or near $x = 0.5$. The extent of ordering seen for a given set of synthesis

and/or annealing conditions may be both kinetically and thermodynamically controlled, and careful further study is needed.

Finally, the determined enthalpies of formation from oxides ($\Delta H_{f,ox}$) and elements (ΔH_f°) at room temperature are summarized in Table 4. Note that the enthalpy of formation of ThSiO_4 obtained from this work, -6.4 ± 5.7 kJ/mol, agrees well with the computational result³⁴, but is inconsistent with the previously measured formation enthalpy value 19.6 ± 2.0 kJ/mol³⁰. This discrepancy may be due to the incomplete dissolution of large coarsely ground thorite single crystals used by Mazeina *et al.*³⁰. Those early experiments did not use gas bubbling and the samples indeed dissolved slowly.

$\Delta H_{f,ox}$ values plotted in Figure 5c are fitted to a quadratic equation,

$$\Delta H_{f,ox} = a' + b' \cdot x + c' \cdot x^2. \quad (5)$$

where $a' = -3.9 \pm 3.9$ kJ/mol, $b' = -93.6 \pm 19.0$ kJ/mol, $c' = 120.1 \pm 17.7$ kJ/mol, and $\text{adj. } R^2 = 0.9467$. The fitted enthalpy of formation curve suggests that the uranothorite phases formed between $x = 0$ and 0.8 are energetically favorable. This is consistent with the formation of these phases in synthesis experiments^{4, 5}, and their relatively common geologic occurrence⁶⁻¹¹. Förster¹¹ and Pointer *et al.*⁸ have documented that most observed uranothorite minerals have 35 ~ 36 mol % U, which is near the minimum of the enthalpy of formation curve (Figure 5c). As the U loading exceeds $x = 0.8$, the enthalpy of formation from oxides becomes positive, suggesting unfavorable formation of uranothorite phases, with coffinite the most unstable phase relative to the oxides by 25.6 ± 3.9 kJ/mol²⁶. This is also consistent with syntheses by Costin *et al.*⁴ that show that, under the same preparation conditions, beyond $x = 0.8$, hardly any U,Th - containing silicate phases were recovered. In addition, between $x = 0.3$ and 0.8, secondary phases such as $\text{Th}_{1-y}\text{U}_y\text{O}_2$ were found to coexist with the synthetic uranothorite phase^{4, 51}, and to become the dominant phases with higher U loadings⁴. Similar trends relating coffinite and uraninite have been found in ore

deposits^{20, 22}. These observations suggest that, with increasing U content, tetravalent uranium prefers to be precipitated in oxide phases rather than in silicate phases from a thermodynamic point of view. In other words, there may be a crossover between the free energy curves of uranothorite and uranothorianite, such that, at intermediate U loading, the former becomes less thermodynamically favorable but both phases can still be formed. With $x > 0.8$, uranothorite formation becomes thermodynamically unfavorable, leaving U - enriched uranothorianite the only stable phase. Thus, besides possible kinetic hindering mechanisms⁴, the increasing metastability of $\text{Th}_{1-x}\text{U}_x\text{SiO}_4$ as a function of uranium content may also explain why the synthesis of high uranium uranothorite or pure coffinite is generally difficult. The thermodynamic data also imply that high uranium uranothorite may follow a similar formation route as coffinite through aqueous dissolution of uraninite and reprecipitation of U in silicate phases^{26, 29}, whereas, synthesis of uranothorite with compositions near the thorite end-member may be possible *via* a direct solid state process from U/Th oxides.

Conclusion

Direct calorimetric experiments on $\text{Th}_{1-x}\text{U}_x\text{SiO}_4$ uranothorite have yielded their standard enthalpies of formation from the constituent oxides and elements. The uranothorite compositions are energetically more stable than their end-members, coffinite and thorite, and show a large negative heat of mixing suggestive of cation ordering for intermediate compositions, which is consistent with crystallographic observations. These results provide a basis for understanding why uranothorite with high U-loadings is metastable relative to a mixture of binary oxides plus quartz.

Acknowledgements

Calorimetric measurements at UC Davis and later data analyses were supported by the Materials Science of Actinides, an Energy Frontier Research Center, funded by the U.S. Department of Energy, Office of Science, Office of Basic Energy Sciences under Award DE-SC0001089. X. G. was also supported by a Seaborg postdoctoral fellowship from the Laboratory Directed Research and Development (LDRD) program, through the G. T. Seaborg Institute, of Los Alamos National Laboratory (LANL), which is operated by Los Alamos National Security LLC, under DOE Contract DE-AC52-06NA25396. The experiments associated to the preparation and characterization of single phase and homogeneous uranothorite solid solutions were supported by the NEEDS Resources program of the CNRS (French National Center for Scientific Research).

Table 1 Elemental analysis of the synthesized uranothorite determined by wavelength dispersive spectroscopy (WDS).

Sample	Th	U	Si	Experimental formula
ThSiO ₄	59.67 ± 1.34 (16.90)*	--	6.75 ± 0.18 (15.79)	ThSiO ₄
ThU1	59.55 ± 1.24 (15.10)	6.80 ± 0.37 (1.84)	7.02 ± 0.18 (16.06)	Th _{0.89} U _{0.11} SiO ₄
ThU2	47.07 ± 1.12 (13.21)	13.11 ± 0.50 (3.59)	6.97 ± 0.18 (16.16)	Th _{0.79} U _{0.21} SiO ₄
ThU4	37.37 ± 0.96 (10.67)	20.79 ± 0.63 (5.79)	6.98 ± 0.18 (16.47)	Th _{0.65} U _{0.35} SiO ₄
ThU7	17.32 ± 0.59 (4.79)	43.63 ± 1.02 (11.75)	7.34 ± 0.19 (16.74)	Th _{0.29} U _{0.71} SiO ₄
ThU8	9.71 ± 0.43 (2.72)	51.28 ± 1.14 (14.00)	7.16 ± 0.19 (16.56)	Th _{0.16} U _{0.84} SiO ₄

* wt. % with at. % in parenthesis. Uncertainty is two standard deviations of the mean.

Table 2 The refined unit cell parameters and molar volume of uranothorite.

Sample	Formula	a (Å)	c (Å)	Volume (Å ³)
ThSiO ₄	ThSiO ₄	7.1568(1)	6.3152(1)	323.46(1)
ThU1	Th _{0.89} U _{0.11} SiO ₄	7.1241(1)	6.3206(1)	320.79(1)
ThU2	Th _{0.79} U _{0.21} SiO ₄	7.1004(1)	6.3121(1)	318.23(1)
ThU4	Th _{0.65} U _{0.35} SiO ₄	7.0697(2)	6.3084(2)	315.29(1)
ThU7	Th _{0.29} U _{0.71} SiO ₄	7.0255(1)	6.2778(1)	309.86(1)
ThU8	Th _{0.16} U _{0.84} SiO ₄	7.0106(1)	6.2706(1)	308.19(1)
USiO ₄	USiO ₄	6.9904(1)	6.2610(1)	305.94(1)

Table 3 Thermochemical cycles for $\text{Th}_{1-x}\text{U}_x\text{SiO}_4$ ($x = 0, 0.11, 0.21, 0.35, 0.71, 0.84$) (based on drop solution calorimetry in molten $2\text{PbO} \cdot \text{B}_2\text{O}_3$ at $802\text{ }^\circ\text{C}$).

Reaction	ΔH (kJ/mol)
<i>Enthalpies of formation of $\text{Th}_{1-x}\text{U}_x\text{SiO}_4$ from the binary oxides ($\Delta H_{f,ox}$) at $25\text{ }^\circ\text{C}$</i>	
(1) $\text{Th}_{1-x}\text{U}_x\text{SiO}_4(\text{s}, 25\text{ }^\circ\text{C}) + x/2\text{O}_2(\text{g}, 802\text{ }^\circ\text{C})$ $\rightarrow x\text{UO}_3(\text{sln}, 802\text{ }^\circ\text{C}) + \text{SiO}_2(\text{sln}, 802\text{ }^\circ\text{C}) + (1-x)\text{ThO}_2(\text{sln}, 802\text{ }^\circ\text{C})$	$\Delta H_1 = \Delta H_{\text{ds}}$
(2) $\text{UO}_2(\text{s}, 25\text{ }^\circ\text{C}) + 1/2\text{O}_2(\text{g}, 802\text{ }^\circ\text{C}) \rightarrow \text{UO}_3(\text{sln}, 802\text{ }^\circ\text{C})$	$\Delta H_2 = -125.21^* \pm 3.41^\dagger(5)^\ddagger_{26,59}$
(3) $\text{ThO}_2(\text{s}, 25\text{ }^\circ\text{C}) \rightarrow \text{ThO}_2(\text{sln}, 802\text{ }^\circ\text{C})$	$\Delta H_3 = 98.1 \pm 1.7(15)^{30}$
(4) $\text{SiO}_2(\text{quartz}, \text{s}, 25\text{ }^\circ\text{C}) \rightarrow \text{SiO}_2(\text{sln}, 802\text{ }^\circ\text{C})$	$\Delta H_4 = 49.9 \pm 0.8(9)^{30}$
(5) $\text{U}(\text{s}, 25\text{ }^\circ\text{C}) + \text{O}_2(\text{g}, 25\text{ }^\circ\text{C}) \rightarrow \text{UO}_2(\text{s}, 25\text{ }^\circ\text{C})$	$\Delta H_5 = -1084.9 \pm 1.0^{64}$
(6) $\text{Th}(\text{s}, 25\text{ }^\circ\text{C}) + \text{O}_2(\text{g}, 25\text{ }^\circ\text{C}) \rightarrow \text{ThO}_2(\text{s}, 25\text{ }^\circ\text{C})$	$\Delta H_6 = -1226.4 \pm 3.5^{64}$
(7) $\text{Si}(\text{s}, 25\text{ }^\circ\text{C}) + \text{O}_2(\text{g}, 25\text{ }^\circ\text{C}) \rightarrow \text{SiO}_2(\text{quartz}, \text{s}, 25\text{ }^\circ\text{C})$	$\Delta H_7 = -910.7 \pm 1.0^{64}$

Enthalpy of mixing of $\text{Th}_{1-x}\text{U}_x\text{SiO}_4$ from USiO_4 and ThSiO_4 :

$$\Delta H_{\text{mix}}(\text{Th}_{1-x}\text{U}_x\text{SiO}_4) = -\Delta H_1 + x\Delta H_{\text{ds}}(\text{USiO}_4)^{26} + (1-x)\Delta H_{\text{ds}}(\text{ThSiO}_4)$$

Enthalpy of formation of $\text{Th}_{1-x}\text{U}_x\text{SiO}_4$ from UO_2 , ThO_2 and SiO_4 :

$$\Delta H_{f,ox}(\text{Th}_{1-x}\text{U}_x\text{SiO}_4) = -\Delta H_1 + x\Delta H_2 + (1-x)\Delta H_3 + \Delta H_4$$

Standard enthalpy of formation of $\text{Th}_{1-x}\text{U}_x\text{SiO}_4$:

$$\Delta H^\circ_f(\text{Th}_{1-x}\text{U}_x\text{SiO}_4) = \Delta H_{f,ox} + x\Delta H_5 + (1-x)\Delta H_6 + \Delta H_7$$

* Average. † Two standard deviations of the average value. ‡ Number of measurements.

Table 4 Enthalpies of drop solution, and enthalpies of formation of $\text{Th}_{1-x}\text{U}_x\text{SiO}_4$ from binary oxides and elements.

Sample	Formula	$\Delta H_{\text{ds}}(\text{kJ/mol})$	$\Delta H_{\text{f,ox}}(\text{kJ/mol})$	$\Delta H_{\text{f}}^{\circ}(\text{kJ/mol})$
ThSiO ₄	ThSiO ₄	154.4 ± 5.4	-6.4 ± 5.7	-2143.5 ± 6.8
ThU1	Th _{0.89} U _{0.11} SiO ₄	137.7 ± 7.0	-14.2 ± 7.2	-2135.8 ± 7.9
ThU2	Th _{0.79} U _{0.21} SiO ₄	118.8 ± 1.2	-17.7 ± 2.1	-2125.1 ± 3.6
ThU4	Th _{0.65} U _{0.35} SiO ₄	91.7 ± 2.5	-21.9 ± 3.1	-2109.5 ± 4.0
ThU7	Th _{0.29} U _{0.71} SiO ₄	-1.7 ± 0.5	-8.9 ± 2.6	-2045.5 ± 3.1
ThU8	Th _{0.16} U _{0.84} SiO ₄	-34.3 ± 3.2	-5.3 ± 4.4	-2023.6 ± 4.6
USiO ₄ ²⁶	USiO ₄	-102.0 ± 3.1 ²⁶	25.6 ± 3.9 ²⁶	-1970.0 ± 4.2 ²⁶

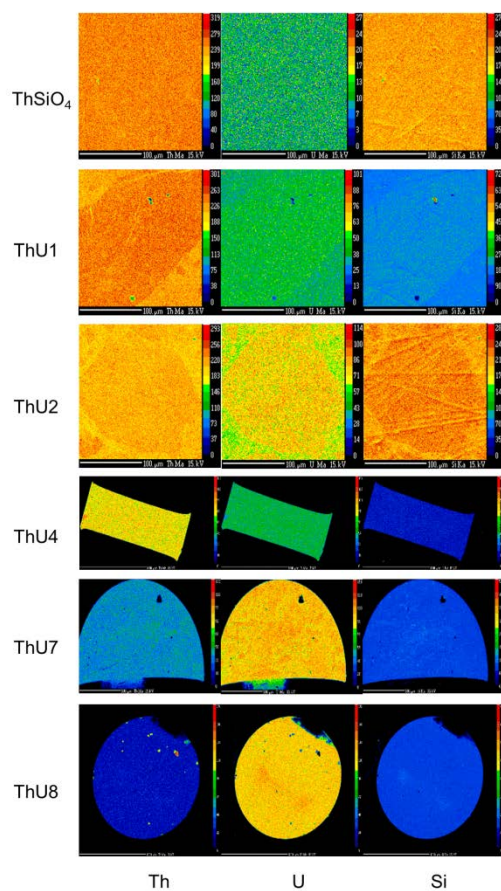


Figure 1. Electron microprobe elemental mapping of Th_{1-x}U_xSiO₄ samples: Mapping of Th on the left, U in the middle, and Si on the right.

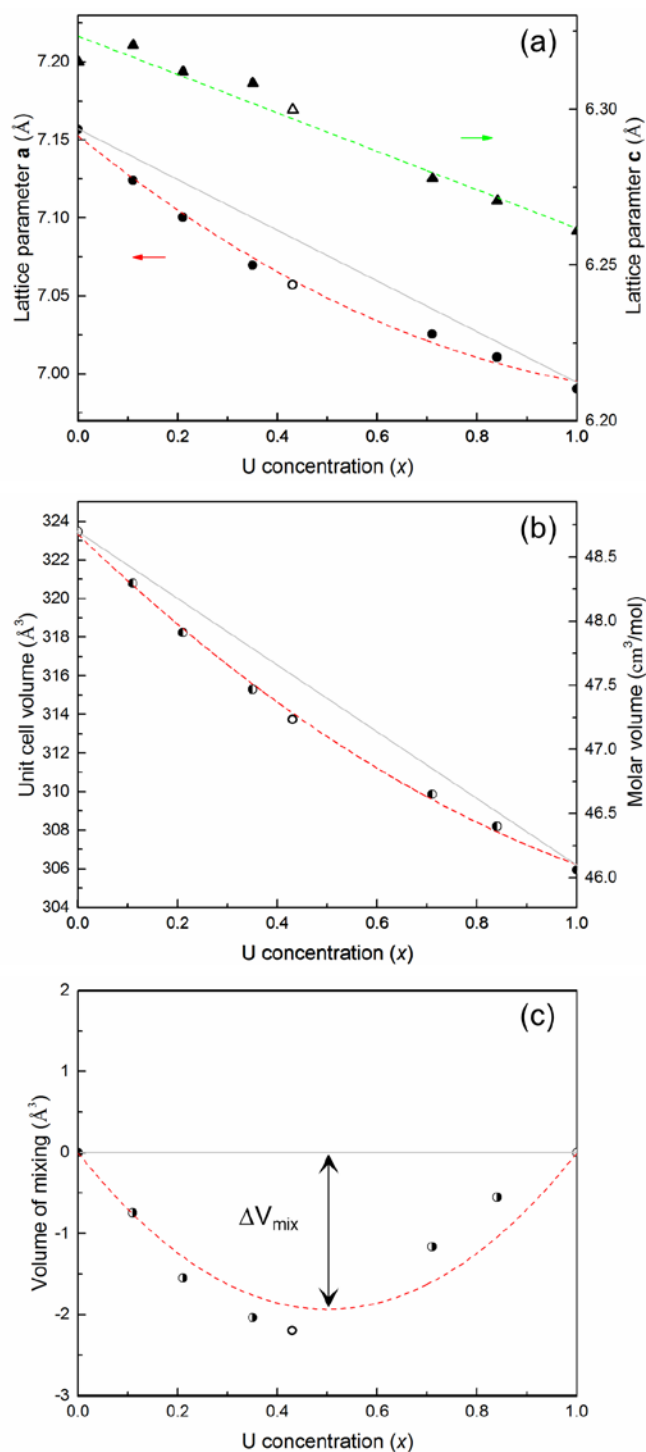


Figure 2. Refined unit cell parameters and molar volume of $\text{Th}_{1-x}\text{U}_x\text{SiO}_4$: (a) Lattice parameter \mathbf{a} fitted by $\mathbf{a} = 7.15 - 0.26x + 0.10x^2$, $\text{adj. } R^2 = 0.9925$, and unit cell parameter \mathbf{c} fitted by $\mathbf{c} = 6.32 - 0.06x$, $\text{adj. } R^2 = 0.9551$; (b) unit cell volume V_{cell} fitted by $V_{\text{cell}} = 323.3 - 24.8x + 7.7x^2$, $\text{adj. } R^2 = 0.9978$ and molar volume; (c) volume of mixing $\Delta V_{\text{mix}} = -7.7 \cdot x(1-x)$. Open circles or triangle at $x = 0.43$ are from Costin *et al.* work⁵¹.

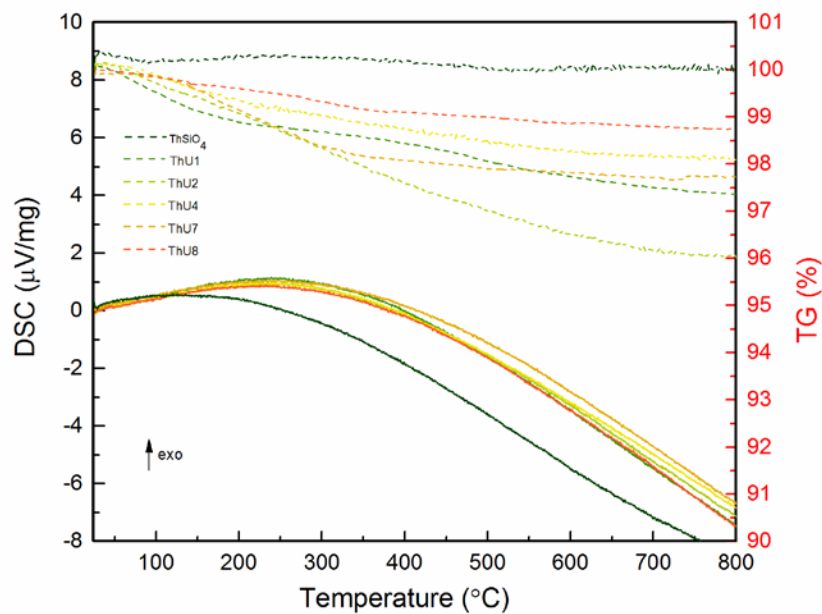


Figure 3. DSC-TG curves of $\text{Th}_{1-x}\text{U}_x\text{SiO}_4$ samples (DSC traces are solid curves, and TG traces are dashed curves).

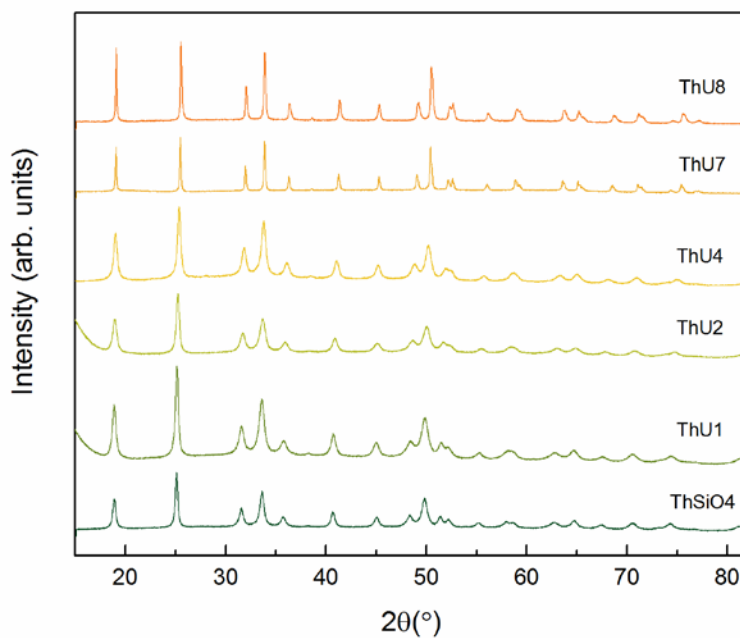


Figure 4. Powder XRD patterns of the $\text{Th}_{1-x}\text{U}_x\text{SiO}_4$ samples recovered after DSC/TG to 800 °C in Ar.

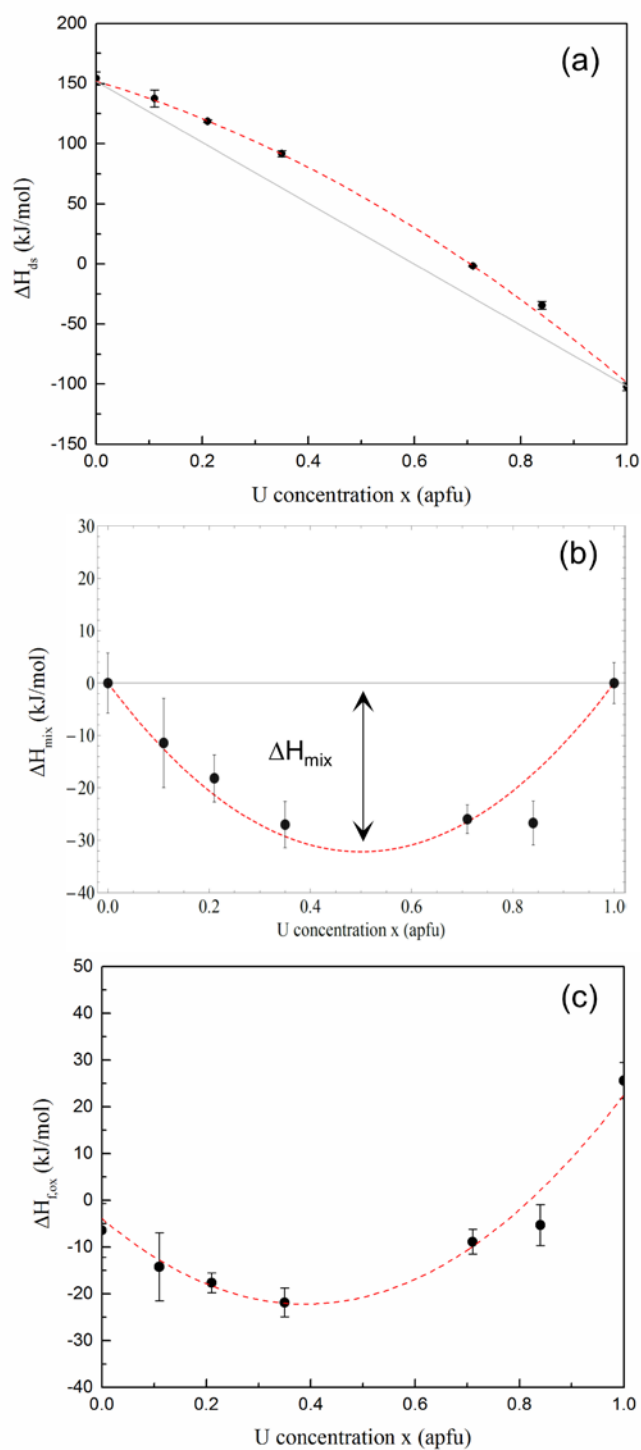


Figure 5. (a) Enthalpies of drop solution, fitted by $\Delta H_{ds} = 152.0 - 131.9 \cdot x - 118.7 \cdot x^2$; (b) Enthalpies of mixing, fitted by $\Delta H_{mix} = -118.7 \cdot x(1-x)$; (c) Enthalpies of formation of $\text{Th}_{1-x}\text{U}_x\text{SiO}_4$ from their binary oxides at 25 °C, fitted by $\Delta H_{f,ox} = -3.9 - 93.6 \cdot x + 120.1 \cdot x^2$.

References

1. Gibb, F. G. F.; Taylor, K. J.; Burakov, B. E., The 'Granite Encapsulation' Route to the Safe Disposal of Pu and Other Actinides. *J. Nucl. Mater.* **2008**, 374, (3), 364-369.
2. Fuchs, L. H.; Gebert, E., X-Ray Studies of Synthetic Coffinite, Thorite and Uranothorites. *Am. Mineral.* **1958**, 43, (3-4), 243-248.
3. Fuchs, L. H.; Hoekstra, H. R., The Preparation and Properties of Uranium(IV) Silicate. *Am. Mineral.* **1959**, 44, (9-10), 1057-1063.
4. Costin, D. T.; Mesbah, A.; Clavier, N.; Dacheux, N.; Poinssot, C.; Szenknect, S.; Ravaux, J., How To Explain the Difficulties in the Coffinite Synthesis from the Study of Uranothorite? *Inorg. Chem.* **2011**, 50, (21), 11117-11126.
5. Szenknect, S.; Costin, D. T.; Clavier, N.; Mesbah, A.; Poinssot, C.; Vitorge, P.; Dacheux, N., From Uranothorites to Coffinite: A Solid Solution Route to the Thermodynamic Properties of USiO₄. *Inorg. Chem.* **2013**, 52, (12), 6957-6968.
6. Ifill, R. O.; Cooper, W. C.; Clark, A. H., Mineralogical Controls on the Oxidative Acid Leaching of Radioactive Phases in Elliot Lake Ores - Brannerite, Uraninite and Uranothorite. *Cim Bulletin* **1987**, 80, (902), 72-72.
7. Pointer, C. M.; Ashworth, J. R.; Ixer, R. A., The Zircon-Thorite Mineral Group in Metasomatized Granite, Ririwai, Nigeria .1. Geochemistry and Metastable Solid-Solution of Thorite and Coffinite. *Mineral. Petrol.* **1988**, 38, (4), 245-262.
8. Pointer, C. M.; Ashworth, J. R.; Ixer, R. A., The Zircon-Thorite Mineral Group in Metasomatized Granite, Ririwai, Nigeria .2. Zoning, Alteration and Exsolution in Zircon. *Mineral. Petrol.* **1988**, 39, (1), 21-37.
9. Lira, R.; Ripley, E. M., Hydrothermal Alteration and Ree-Th Mineralization at the Rodeo-De-Los-Molles Deposit, Las-Chacras-Batholith, Central Argentina. *Contrib. Mineral. Petrol.* **1992**, 110, (2-3), 370-386.
10. Sharma, G. S.; Purohit, R. K.; Roy, M.; Sengupta, B.; Singh, J., Geochemistry and Petrography of U-Th-Y Mineralisation in Alkali Feldspar Granite (Alaskite) Dykes Around Dhanota, Mahendragarh District, Haryana, India. *J Geol. Soc. India* **2000**, 55, (2), 189-196.
11. Forster, H. J., Composition and Origin of Intermediate Solid Solutions in the System Thorite-xenotime-zircon-coffinite. *Lithos* **2006**, 88, (1-4), 35-55.
12. Stieff, L. R.; Stern, T. W.; Sherwood, A. M., Preliminary Description of Coffinite - New Uranium Mineral. *Science* **1955**, 121, (3147), 608-609.
13. Staatz, M. H.; Brownfield, I. K. *X-ray diffraction mineral identification charts for use in studies of uranium, thorium, and rare-earth deposits*; 82-280; 1982.
14. Burakov, B. E.; Anderson, E. B.; Zamoryanskaya, M. V.; Yagovkina, M. A.; Strykanova, E. E.; Nikolaeva, E. V., Synthesis and Study of (239)Pu-doped Ceramics Based on Zircon, (Zr,Pu)SiO(4), and Hafnon, (Hf,Pu)SiO(4). *Scientific Basis for Nuclear Waste Management Xxiv* **2000**, 663, 307-313.
15. Speer, J. A., Orthosilicates. The Actinide Orthosilicates. *Rev. Mineral.* **1980**, 5, (1), 113-35.
16. Grover, V.; Tyagi, A. K., Preparation and Bulk Thermal Expansion Studies in M_{1-x}Ce_xSiO₄ (M = Th, Zr) System, and Stabilization of Tetragonal ThSiO₄. *J. Alloy. Compd.* **2005**, 390, (1-2), 112-114.
17. Smits, G., (U, Th)-Bearing Silicates in Reefs of the Witwatersrand, South-Africa. *Can. Mineral.* **1989**, 27, 643-655.

18. Hansley, P. L.; Fitzpatrick, J. J., Compositional and Crystallographic Data on Ree-Bearing Coffinite from the Grants Uranium Region, Northwestern New-Mexico. *Am Mineral.* **1989**, 74, (1-2), 263-270.
19. Janeczek, J.; Ewing, R. C., Mechanisms of Lead Release from Uraninite in the Natural Fission Reactors in Gabon. *Geochim. Cosmochim. Acta.* **1995**, 59, (10), 1917-1931.
20. Fayek, M.; Janeczek, J.; Ewing, R. C., Mineral Chemistry and Oxygen Isotopic Analyses of Uraninite, Pitchblende and Uranium Alteration Minerals from the Cigar Lake Deposit, Saskatchewan, Canada. *Appl. Geochem.* **1997**, 12, (5), 549-565.
21. Jensen, K. A.; Ewing, R. C., The Okelobondo Natural Fission Reactor, Southeast Gabon: Geology, Mineralogy, and Retardation of Nuclear-reaction Products. *Geol. Soc. Am. Bull.* **2001**, 113, (1), 32-62.
22. Fayek, M.; Harrison, T. M.; Ewing, R. C.; Grove, M.; Coath, C. D., O and Pb Isotopic Analyses of Uranium Minerals by Ion Microprobe and U-Pb Ages from the Cigar Lake Deposit. *Chem. Geol.* **2002**, 185, (3-4), 205-225.
23. Clavier, N.; Szenknect, S.; Costin, D. T.; Mesbah, A.; Ravaux, J.; Poinssot, C.; Dacheux, N., Purification of Uranothorite Solid Solutions from Polyphase Systems. *J. Nucl. Mater.* **2013**, 441, (1-3), 73-83.
24. Labs, S.; Hennig, C.; Weiss, S.; Curtius, H.; Zanker, H.; Bosbach, D., Synthesis of Coffinite, $USiO_4$, and Structural Investigations of $U_xTh_{(1-x)}SiO_4$ Solid Solutions. *Environ. Sci. Tech.* **2014**, 48, (1), 854-860.
25. Mesbah, A.; Szenknect, S.; Clavier, N.; Lozano-Rodriguez, J.; Poinssot, C.; Den Auwer, C.; Ewing, R. C.; Dacheux, N., Coffinite, $USiO_4$, Is Abundant in Nature: So Why Is It So Difficult To Synthesize? *Inorg. Chem.* **2015**, 54, (14), 6687-6696.
26. Guo, X.; Szenknect, S.; Mesbah, A.; Labs, S.; Clavier, N.; Poinssot, C.; Ushakov, S. V.; Curtius, H.; Bosbach, D.; Ewing, R. C.; Burns, P. C.; Dacheux, N.; Navrotsky, A., Thermodynamics of Formation of Coffinite, $USiO_4$. *Proc. Natl. Acad. Sci. U.S.A.* **2015**, 112, (21), 6551-6555.
27. Kleykamp, H., Selection of Materials as Diluents for Burning of Plutonium Fuels in Nuclear Reactors. *J. Nucl. Mater.* **1999**, 275, (1), 1-11.
28. Ewing, R. C.; Lutze, W.; Weber, W. J., Zircon - a Host-Phase for the Disposal of Weapons Plutonium. *J. Mater. Res.* **1995**, 10, (2), 243-246.
29. Szenknect, S.; Mesbah, A.; Cordara, T.; Clavier, N.; Brau, H. P.; Le Goff, X.; Poinssot, C.; Ewing, R. C.; Dacheux, N., First Experimental Determination of the Solubility Constant of Coffinite. *Geochim. Cosmochim. Acta.* **2016**, 181, 36-53.
30. Mazeina, L.; Ushakov, S. V.; Navrotsky, A.; Boatner, L. A., Formation Enthalpy of $ThSiO_4$ and Enthalpy of the Thorite \rightarrow Huttonite Phase Transition. *Geochim. Cosmochim. Acta.* **2005**, 69, 4675-4683.
31. Clavier, N.; Szenknect, S.; Costin, D. T.; Mesbah, A.; Poinssot, C.; Dacheux, N., From thorite to coffinite: A Spectroscopic Study of $Th_{1-x}U_xSiO_4$ Solid Solutions. *Spectrochim. Acta. A* **2014**, 118, 302-307.
32. Ushakov, S. V.; Gong, W.; Yagovkina, M. M.; Helean, K. B.; Lutze, W.; Ewing, R. C., Solid solutions of Ce, U, and Th in zircon. *Environmental Issues and Waste Management Technologies in the Ceramic and Nuclear Industries Iv* **1999**, 93, 357-363.
33. Burakov, B. E.; Hanchar, J. M.; Zamoryanskaya, M. V.; Garbuzov, V. M.; Zirlin, V. A., Synthesis and Investigation of Pu-doped Single Crystal Zircon, $(Zr, Pu)SiO_4$. *Radiochim. Acta* **2002**, 90, (2), 95-97.
34. Ferriss, E. D. A.; Ewing, R. C.; Becker, U., Simulation of Thermodynamic Mixing Properties of Actinide-containing Zircon Solid Solutions. *Am. Mineral.* **2010**, 95, (2-3), 229-241.

35. Janeczek, J.; Ewing, R. C., Coffinitization - A Mechanism for the Alteration of Uranium Dioxide under Reducing Conditions. *Mater. Res. Soc. Symp. Proc.* **1992**, 257, 497.
36. Janeczek, J.; Ewing, R. C., Dissolution and Alteration of Uraninite under Reducing Conditions. *J. Nucl. Mater.* **1992**, 190, 157-73.
37. Janeczek, J.; Ewing, R. C.; Oversby, V. M.; Werme, L. O., Uraninite and UO₂ in Spent Nuclear Fuel: A Comparison. *J. Nucl. Mater.* **1996**, 238, (1), 121-130.
38. Savary, V.; Pagel, M., The Effects of Water Radiolysis on Local Redox Conditions in the Oklo, Gabon, Natural Fission Reactors 10 and 16. *Geochim. Cosmochim. Acta.* **1997**, 61, (21), 4479-4494.
39. Bros, R.; Hidaka, H.; Kamei, G.; Ohnuki, T., Mobilization and Mechanisms of Retardation in the Oklo Natural Reactor Zone 2 (Gabon) - Inferences from U, REE, Zr, Mo and Se Isotopes. *Appl. Geochem.* **2003**, 18, (12), 1807-1824.
40. Amme, M.; Wiss, T.; Thiele, H.; Boulet, P.; Lang, H., Uranium Secondary Phase Formation during Anoxic Hydrothermal Leaching Processes of UO₂ Nuclear Fuel. *J. Nucl. Mater.* **2005**, 341, (2-3), 209-223.
41. Grambow, B., Nuclear Waste Glasses - How Durable? *Elements* **2006**, 2, (6), 357-364.
42. Finch, C. B.; Clark, G. W.; Harris, L. A., Thorite-Huttonite Phase Transformation as Determined by Growth of Synthetic Thorite + Huttonite Single Crystals. *Am. Mineral.* **1964**, 49, (5-6), 782-785.
43. Taylor, M.; Ewing, R. C., Crystal-Structures of ThSiO₄ Polymorphs - Huttonite and Thorite. *Acta Crystallogr. B* **1978**, 34, (Apr), 1074-1079.
44. Ewing, R. C., Nuclear Waste Forms for Actinides. *Proc. Natl. Acad. Sci. U.S.A.* **1999**, 96, (7), 3432-3439.
45. Yudinsev, S. V.; Stefanovsky, S.; Ewing, R. C., Actinide Host Phases as Radioactive Waste Forms. In *Structural Chemistry of Inorganic Actinide Compounds*, Krivovichev, S. V.; Tananaev, I., Eds. Elsevier 2007; pp 457-490.
46. Lumpkin, G. R., Ceramic Waste Forms for Actinides. *Elements* **2006**, 2, (6), 365-372.
47. Dacheux, N.; Brandel, V.; Genet, M., Synthesis and Properties of Uranium Chloride Phosphate Tetrahydrate: UClPO₄·4H₂O. *New J. Chem.* **1995**, 19, (10), 1029-1036.
48. Dacheux, N.; Brandel, V.; Genet, M., Synthèse et caractérisation de l'orthophosphate d'uranium a valence mixte: U(UO₂)(PO₄)₂. *New J. Chem.* **1995**, 19, (1), 15-26.
49. Dacheux, N.; Brandel, V.; Genet, M.; Bak, K.; Berthier, C., Solid Solutions of Uranium and Thorium Phosphates: Synthesis, Characterization and X-ray Photoelectron Spectroscopy. *New J. Chem.* **1996**, 20, (3), 301-310.
50. Hoekstra, H. R.; Fuchs, L. H., Synthesis of Coffinite-USiO₄. *Science* **1956**, 123, (3186), 105-105.
51. Costin, D. T.; Mesbah, A.; Clavier, N.; Szenknect, S.; Dacheux, N.; Poinssot, C.; Ravaux, J.; Brau, H. P., Preparation and Characterization of Synthetic Th_{0.5}U_{0.5}SiO₄ Uranothorite. *Prog. Nucl. Energ.* **2012**, 57, 155-160.
52. Guo, X.; Ushakov, S. V.; Labs, S.; Curtius, H.; Bosbach, D.; Navrotsky, A., Energetics of Metastudtite and Implications for Nuclear Waste Alteration. *Proc. Natl. Acad. Sci. U.S.A.* **2014**, 111, (50), 17737-17742.
53. Navrotsky, A., Progress and New Directions in High-Temperature Calorimetry. *Phys. Chem. Miner.* **1977**, 2, (1-2), 89-104.
54. Navrotsky, A., Progress and New Directions in High Temperature Calorimetry Revisited. *Phys. Chem. Miner.* **1997**, 24, (3), 222-241.
55. Navrotsky, A., Progress and New Directions in Calorimetry: A 2014 Perspective. *J. Am. Ceram. Soc.* **2014**, 97, (11), 3349-3359.

56. Navrotsky, A.; Rapp, R. P.; Smelik, E.; Burnley, P.; Circone, S.; Chai, L.; Bose, K., The Behavior of H₂O and CO₂ in High-Temperature Lead Borate Solution Calorimetry of Volatile-Bearing Phases. *Am. Mineral.* **1994**, 79, (11-12), 1099-1109.
57. Guo, X.; Tiferet, E.; Qi, L.; Solomon, J. M.; Lanzirotti, A.; Newville, M.; Engelhard, M. H.; Kukkadapu, R. K.; Wu, D.; Ilton, E. S.; Asta, M.; Sutton, S.; Xu, H.; Navrotsky, A., U(V) in Metal Uranates: A Combined Experimental and Theoretical Study of MgUO₄, CrUO₄ and FeUO₄. *Dalton Trans.* **2016**, 45, (11), 4622-4632.
58. Guo, X.; Wu, D.; Xu, H.; Burns, P. C.; Navrotsky, A., Thermodynamic Studies of Studtite Thermal Decomposition Pathways via Amorphous Intermediates UO₃, U₂O₇, and UO₄. *J. Nucl. Mater.* **2016**, 478, 158-163.
59. Guo, X.; Navrotsky, A.; Kukkadapu, R. K.; Engelhard, M. H.; Lanzirotti, A.; Newville, M.; Ilton, E. S.; Sutton, S.; Xu, H., Structure and Thermodynamics of Uranium Containing Iron Garnets *Geochim. Cosmochim. Acta.* **2016**, 189, 269-281.
60. Guo, X.; Lipp, C.; Tiferet, E.; Lanzirotti, A.; Newville, M.; Engelhard, M. H.; Wu, D.; Ilton, E. S.; Sutton, S.; Xu, H.; Burns, P. C.; Navrotsky, A., Structure and thermodynamic stability of UTa₃O₁₀, a U(V) - bearing compound. *Dalton Trans.* **2016**, DOI: 10.1039/c6dt02843h.
61. Shannon, R. D., Revised Effective Ionic-Radii and Systematic Studies of Interatomic Distances in Halides and Chalcogenides. *Acta Crystallogr. A* **1976**, 32, (Sep1), 751-767.
62. Davies, P. K.; Navrotsky, A., Quantitative Correlations of Deviations from Ideality in Binary and Pseudobinary Solid-Solutions. *J. Solid State Chem.* **1983**, 46, (1), 1-22.
63. Keller, C., Untersuchungen über die germanate und silikate des typs ABO₄ der vierwertigen elemente thorium bis americium. *Nukleonik* **1963**, 5, 41-48.
64. Robie, R. A.; Hemingway, B. S., *Thermodynamic properties of minerals and related substances at 298.15 K and 1 bar pressure and at higher temperatures.* 1995; Vol. 2131.